

Article

Investigations on the Reverse Flotation of Quartz/Hematite Using Pullulan as a Novel Depressant

Wenjie Han *, Yimin Zhu *, Zhichao Shuai, Jie Liu and Yanjun Li

College of Resources and Civil Engineering, Northeastern University, Shenyang 110819, China

* Correspondence: hanwenjie@stumail.neu.edu.cn (W.H.); zhuyimin@mail.neu.edu.cn (Y.Z.)

Abstract: The traditional hematite depressant starch has the disadvantages of poor solubility and high viscosity. In this study, a novel hematite depressant, pullulan, with better performance and flotation effect than starch was found. The structure, molecular weight and viscosity of pullulan were determined for its characterization. The results of flotation tests revealed that the flotation separation of hematite-quartz by pullulan was better than that of starch for hematite-quartz. The selective depression mechanism of pullulan on hematite was studied by contact angle measurement, zeta potential measurement, FT-IR analyses and XPS analyses. Overall, the weak adsorption of pullulan on quartz did not affect the adsorption of DOPA on the quartz surface. However, it was adsorbed strongly on hematite surface and hindered the adsorption of DOPA. This selective adsorption led to a much greater hydrophobicity of quartz than hematite in the reverse flotation, resulting in the separation of quartz and hematite. Pullulan was adsorbed by chemical bonding between its hydroxyl group and iron sites on the hematite surface. Thus, compared with starch, pullulan was easy to dissolve in water, had low viscosity and good flotation effect, so it was a better hematite depressant.

Keywords: pullulan; depressant; hematite; quartz; flotation



Citation: Han, W.; Zhu, Y.; Shuai, Z.; Liu, J.; Li, Y. Investigations on the Reverse Flotation of Quartz/Hematite Using Pullulan as a Novel Depressant. *Metals* **2023**, *13*, 550. <https://doi.org/10.3390/met13030550>

Academic Editor: Antoni Roca

Received: 6 February 2023

Revised: 27 February 2023

Accepted: 7 March 2023

Published: 9 March 2023



Copyright: © 2023 by the authors. Licensee MDPI, Basel, Switzerland. This article is an open access article distributed under the terms and conditions of the Creative Commons Attribution (CC BY) license (<https://creativecommons.org/licenses/by/4.0/>).

1. Introduction

Reverse flotation is considered to be one of the most effective methods for removing gangue minerals from iron oxide minerals. In China, it is usually used in combination with magnetic separation in plants to enrich iron oxide minerals [1,2]. The ore sample entering the flotation operation is a magnetic separation concentrate. Reverse cationic flotation has the advantages of low flotation temperature and a simple reagent system, and occupies an important position in the field of iron oxide mineral flotation, where selective suppression of iron oxide minerals is very important [3].

The flotation separation of hematite and quartz usually adopts a reverse flotation process, that is, hematite is depressed to collect quartz [4]. Therefore, depressants play an important role in reverse flotation of iron ore. Starch is a traditional hematite depressant [2]. The research and development of new hematite depressants are mainly based on polysaccharide compounds, such as carboxymethyl chitosan, curdlan, fungal cellulase, guar gum and CMC [5–9]. In addition, HPAM, tannin, polymaleic anhydride-triethylenetetramine (PMTA) and humic acid are also used as hematite depressants [4,10,11]. However, starch needs to be heated or alkali in preparation, which requires additional energy consumption. Moreover, the viscosity of aqueous solutions such as starch, curdlan, guar gum and CMC are high, and according to the feedback of workers on site, high viscosity will lead to pipe clogging and filtering difficulties [12]. In addition, the current studies have not systematically characterized information such as molecular weight and viscosity of the inhibitors. This was detrimental to the promotion and application of the inhibitors and the reproducibility of the experiments. In this paper, the water-soluble carbohydrate polymer pullulan was used as an inhibitor of hematite.

Pullulan polysaccharide is a kind of water-soluble microbial polysaccharide produced by the fermentation of *blastomyces breviflora* [13]. The polysaccharide is a straight chain polysaccharide polymerized from the α -1, 4-glycosidic bonded malt trisose repeat unit by linkages through the α -1, 6-glycosidic bond, and has a molecular weight of 20,000–2 million [14].

Pullulan has been studied and applied in many fields. In mineral processing, pullulan was applied as selective depressant of galena-sphalerite and chalcopyrite-talc [15,16]. At present, there has been no study on the application and mechanism of pullulan in a selective hematite depressant role in quartz-hematite reverse flotation. Pullulan was used as a depressant of hematite in this study. The effectiveness of pullulan on the separation of quartz/hematite reverse flotation was verified by flotation tests. The depression mechanism was studied by contact angle, zeta potential, FT-IR and XPS analyses.

2. Materials and Methods

2.1. Minerals and Reagents

The single minerals utilized in this research were all derived from Anshan, China. First, a batch of high purity hematite and quartz was hand-picked, then crushed, ground and screened to obtain powder products of different grain sizes. The products of $-74 \mu\text{m} + 45 \mu\text{m}$ were used for the flotation test and XPS test. The products of $-45 \mu\text{m}$ were used for FT-IR tests. The products of $5 \mu\text{m}$ were used for zeta potential tests. For $1 \times 2 \times 0.5 \text{ mm}$ block ore, the contact angle tests were carried out after polishing one side. After chemical analyses, the content of SiO_2 in quartz samples was 99.25%, the grade of TFe in hematite samples was 69.26%, and the content of FeO was only 0.17%. Therefore, the purity of the single minerals could be satisfied with the experimental requirements.

The reagents used in this study were dodecoxypropylamine (DOPA, collector), pullulan (depressant), starch, sodium hydroxide (pH adjuster), hydrochloric acid (pH adjuster), potassium bromide, potassium chloride. DOPA was purchased from Tianmen Hengchang Chemical Co., LTD. Pullulan was purchased from Plum Biotechnology Group Co., LTD. All other reagents were purchased from Tianjin Kemiou Co., LTD. All reagents were chemically pure except potassium bromide which was spectral pure. Pullulan was dissolved directly in cold water to prepare an aqueous solution. Starch was mixed with NaOH (20% of the starch mass) and heated in a water bath ($85 \text{ }^\circ\text{C}$) for 15 min to obtain the starch solution.

2.2. Flotation Tests

Flotation tests included micro-flotation tests and mineral mixture flotation tests. The appropriate amount of single mineral (2 g) or mineral mixture (50 g) was added to the flotation cells with 30 mL or 150 mL of deionized water, respectively, according to the process shown in Figure 1. Then the pulp pH was adjusted, the depressant (pullulan and starch) was added, and the collector (DOPA) was added. All the above actions were performed at 2 min intervals. In single mineral tests, the flotation recovery could be obtained after the foam product was filtered, dried and weighed. The mineral mixture flotation test was a reverse flotation test of iron ore; the froth product was tailings and the product in the flotation cell was iron ore concentrate. The total iron content (TFe grade) of the product was obtained by chemical analysis after drying. The flotation machine used for the test was an XFG-II flotation machine. Each experiment was carried out three times and the average was taken as the final result.

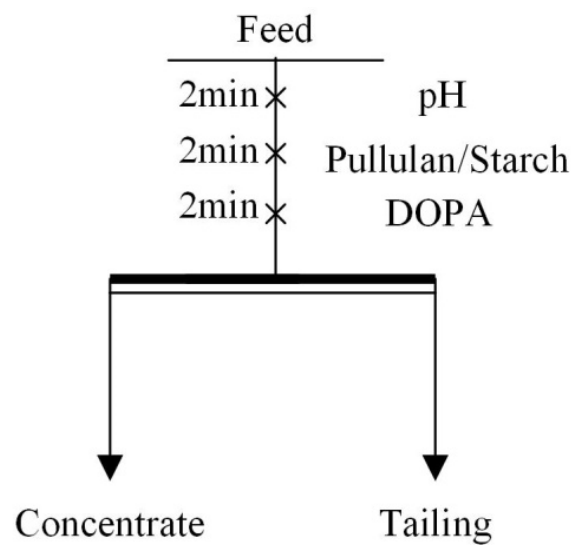


Figure 1. Flowsheet of flotation experiments.

2.3. Molecular Weight Measurements

The relative molecular weight of samples was measured by gel permeation chromatography (GPC). A Pl-gpc 50 gel permeation chromatograph was used for measurement. The selected mobile phase was the aqueous phase. The data obtained were plotted and analyzed by Origin software.

2.4. Viscosity Measurements

The viscosity of pullulan and starch solution was measured by NDJ-1 rotary viscometer (Shanghai Nyirun Intelligent Technology Co., LTD, Shanghai, China). Pullulan was dissolved directly in cold water to prepare an aqueous solution of different concentrations. Rotor 0 was selected for measurement at a speed of 60 r/min.

2.5. Contact Angle Measurements

The contact angle was measured by Dataphysics DCAT21 (Herner, Berlin, Germany) contact angle measuring instrument. The minerals were polished into rectangular blocks of $1 \times 2 \times 0.5$ mm and one side was polished. The block samples were soaked in different reagent solutions for 30 min and then taken out to dry at room temperature. Each test was performed 5 times and the results were averaged.

2.6. Zeta Potential Measurements

Zeta potential on the mineral surface was measured by a Malvern Zetasizer Nano ZS90 zeta potential analyzer (Malvern Company, Grovewood, UK). The 1×10^{-3} mol/L potassium chloride solution was used as the background solution during measurements. Hematite and quartz were treated in different reagent solutions and their supernatant was measured. The measurements were repeated three times; the average value was taken and recorded.

2.7. FT-IR Measurements

FT-IR analyses were performed with a Nexus 670 FT-IR analyzer (Nicolet Corporation, Waltham, MA, USA). The infrared scanning range was 400 to 4000 cm^{-1} . The samples were treated with pullulan and dried at room temperature. With potassium bromide as the sampling background, the mineral and potassium bromide were mixed and pressed. The product was then analyzed to collect its infrared spectrum.

2.8. XPS Measurements

XPS analyses were performed by ThermoFisher K-Alpha spectrometer (Thermo, Waltham, MA, USA). The technical parameters of the measurements were as follows: 1. X-ray source—Al K α micro-concentrated monochromator (Thermo, Waltham, MA, USA)—spot size (5 μm steps 30–400 μm); 2. Ion gun—energy range 100–4000 eV; 3. Vacuum was generally 8×10^{-8} and the angle of incidence was 90 degrees.

3. Results and Discussion

3.1. The Characterization of Pullulan

3.1.1. FT-IR Spectroscopy

The structure of pullulan was characterized by infrared spectroscopy. The FT-IR spectra of pullulan are shown in Figure 2. The information on the conformation for the glucopyranosyl unit in the polysaccharide was available in the region 1000–700 cm^{-1} . The peaks at 847.08 cm^{-1} and 764.64 cm^{-1} indicated that the pullulan has the $4C_1$ chair conformation [17]. The absorption peak at 1021.47 cm^{-1} was attributed to the vibration of the C-O bond at glucose C4 [18]. The band at 1369.21 cm^{-1} was considered to be the bending vibration of the primary C-OH group at the C6 position [19]. The band at 1641.90 cm^{-1} was considered to be the valence vibrations of the C-O-C bond and the glycoside bridge [20]. The wide-band of 3432.19 cm^{-1} was caused by the stretching vibration of -OH in carbohydrates [21].

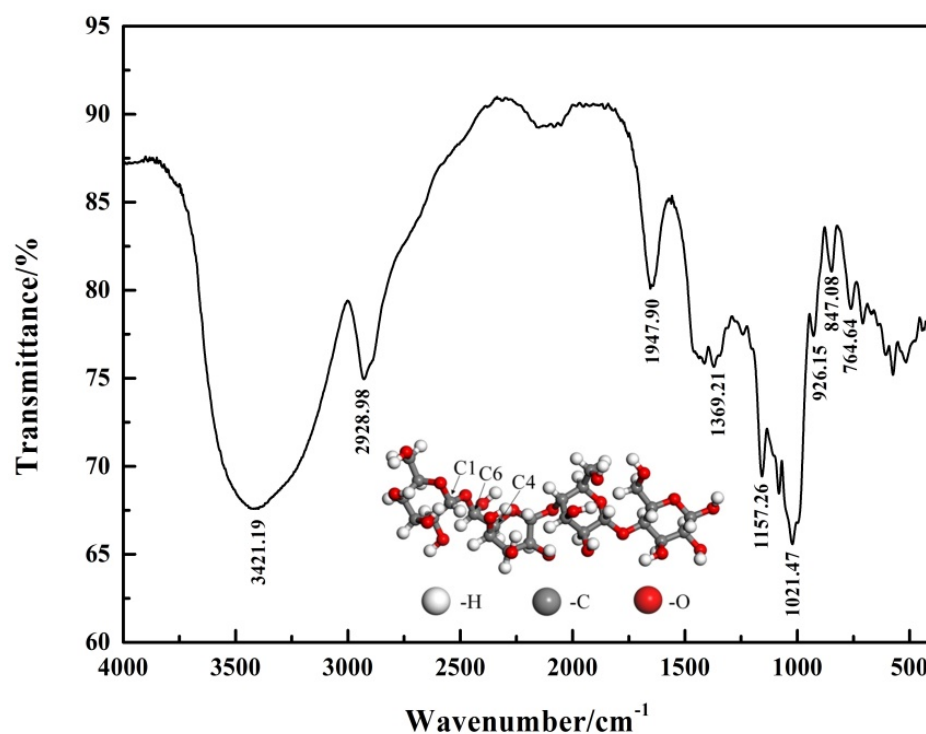


Figure 2. FT-IR spectrum of pullulan.

3.1.2. Molecular Weight Tests

The molecular weight of polysaccharide depressants had a significant effect on their adsorption and inhibition on the mineral surface [22,23]. Figure 3 shows the molecular weight distribution of the pullulan used in this paper. The pullulan molecular weight had two distributions, mainly distribution 1. Distribution 1 had a number average molecular weight (Mn) of 24,608, a heavy average weight (Mw) of 112,500, and a peak molecular weight (MP) of 108,575. Distribution 2 had a number average molecular weight (Mn) of 980, a heavy average weight (Mw) of 1455, and a peak molecular weight (MP) of 1358.

The determined value of the molecular weight will help the application and promotion of pullulan in flotation industrialization in the future.

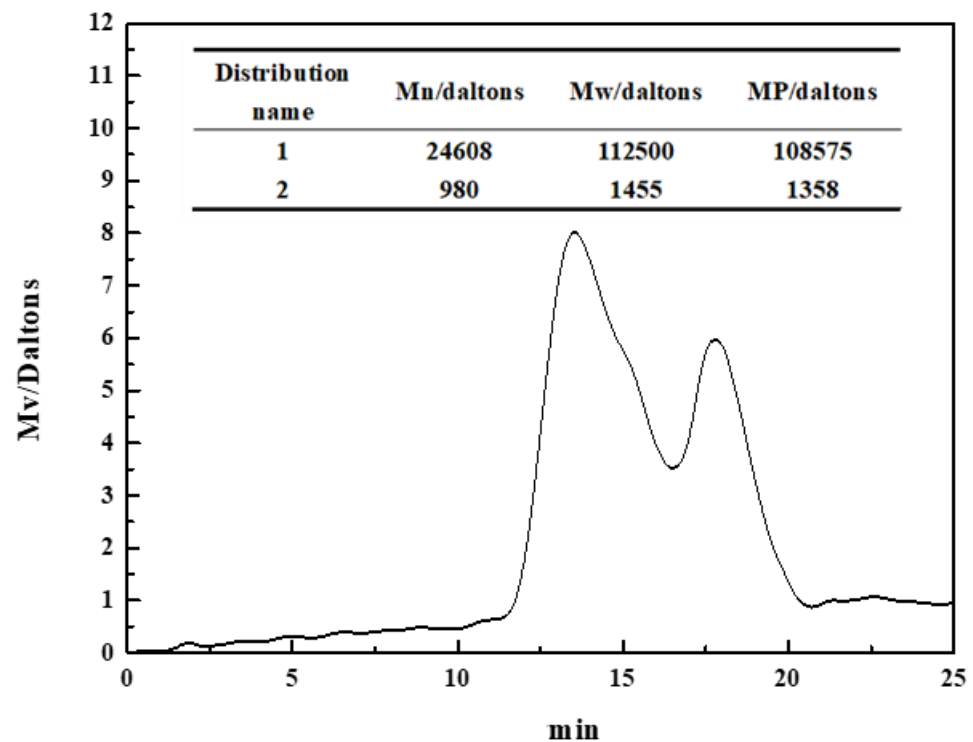


Figure 3. The molecular weight of pullulan.

3.1.3. Viscosity Measurement Results

According to the feedback of workers on the flotation site, starch tended to block pipes due to its high viscosity. In addition, the high viscosity of the pulp makes subsequent dewatering operations of the flotation concentrate more difficult [12]. As can be seen from Figure 4, the viscosity of starch was always higher than that of pullulan, and its viscosity also increased with the increase of starch concentration. In contrast, the viscosity of pullulan did not change significantly as its concentration increased. This demonstrated that from a process point of view, pullulan was more appropriate for the industrial production as a depressant.

3.2. Micro-Flotation Results

The floatability of quartz and hematite with DOPA as collector and without depressant is shown in Figure 5a,b. For the purpose of comparison, the recovery of quartz and hematite in the single mineral test was the percentage of the froth product to the total mass. In Figure 5a, the effect of pH on the flotation recovery of quartz and hematite was investigated under the DOPA concentration of 10 mg/L. The flotation recovery of quartz remained stable at about 95% at pH 7–10. The flotation recovery of quartz dropped sharply to 2.14% at pH 12, with almost total loss of floatability. The flotation recovery of hematite had the same trend as that of quartz, but was generally lower than that of quartz. The flotation recovery of hematite remained stable at about 60% at pH 7–11. The flotation recovery of hematite dropped sharply to 0.60% at pH 12, with almost loss of floatability. This was due to the presence of amine collectors in molecular form at pH 12, resulting in a loss of their collector ability [24,25]. Figure 5b shows the changes of quartz and hematite flotation recovery with the increase of DOPA concentration at pH 9. When DOPA concentration was 10 mg/L, the flotation recovery rates of quartz and hematite were 97.11% and 68.56%, respectively. From the results, it can be seen that, although there were some differences

between hematite and quartz in floatability, it was necessary to add depressants during the flotation separation.

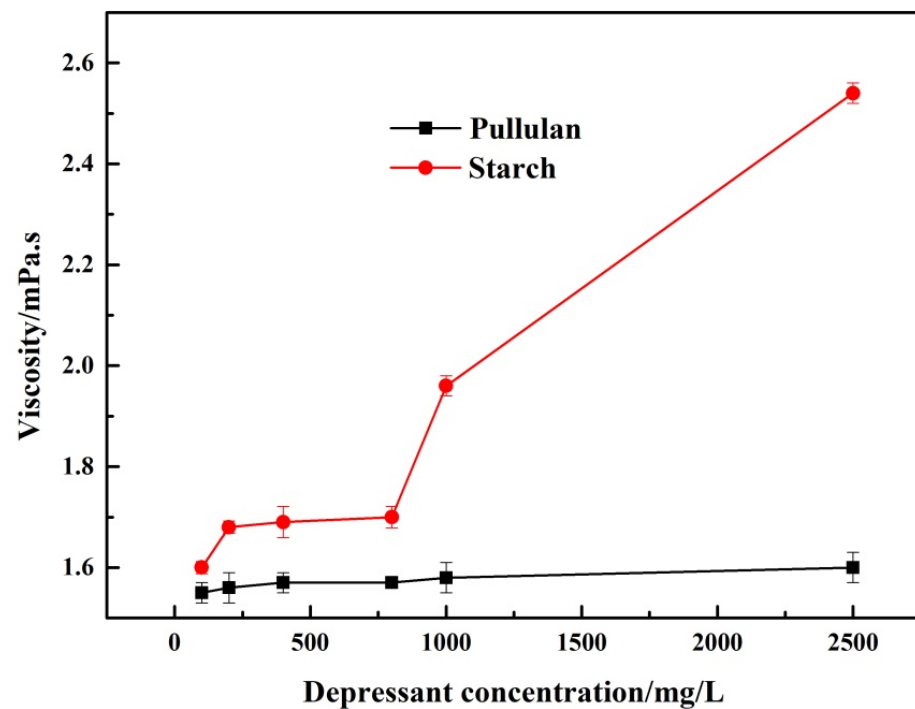


Figure 4. The viscosity of pullulan and starch.

Figure 5c,d show the effect of pullulan and conventional depressant starch on the floatability of quartz and hematite. As shown in Figure 5c, the hematite flotation recovery was lower than 2% in the range of pH 7–12 after the addition of pullulan (30 mg/L) while at pH 7–11, the flotation recovery of quartz remained above 90% and was not affected by pullulan. At pH 12, the flotation recovery of quartz decreased sharply to 1.52% due to the failure of the collector. Figure 5d shows the changes of quartz and hematite flotation recovery with the increase of pullulan and starch concentration at pH 9. With the increase of pullulan and starch concentration, quartz flotation recovery was not affected. With the increase of pullulan and starch concentration, the flotation recovery of hematite decreased gradually, and the decline rate of pullulan was slightly higher than that of starch. From the results, it can be seen that pullulan increased the difference in the floatability of quartz and hematite. Pullulan was a superior hematite depressant than starch.

The above results demonstrated that pullulan, as a depressant of hematite, widens the floatability difference between quartz and hematite. Figure 6 shows the TFe grade and recovery of iron concentrate obtained from mineral mixture tests. Without the addition of depressant, the TFe grade of iron concentrate was increased from 34.68% to 60.1% but the iron recovery was only 28.75%. Most of the iron was lost. With the addition of depressant, the grade of iron concentrate increased to 65.35% (pullulan) and 64.51% (starch) and the iron recovery was 90.68% (pullulan) and 90.18% (starch), respectively. Pullulan was soluble in cold water, as opposed to starch, which required gelatinization. The flotation effect of pullulan was also slightly better than that of starch. Therefore, pullulan was a superior hematite depressant than starch.

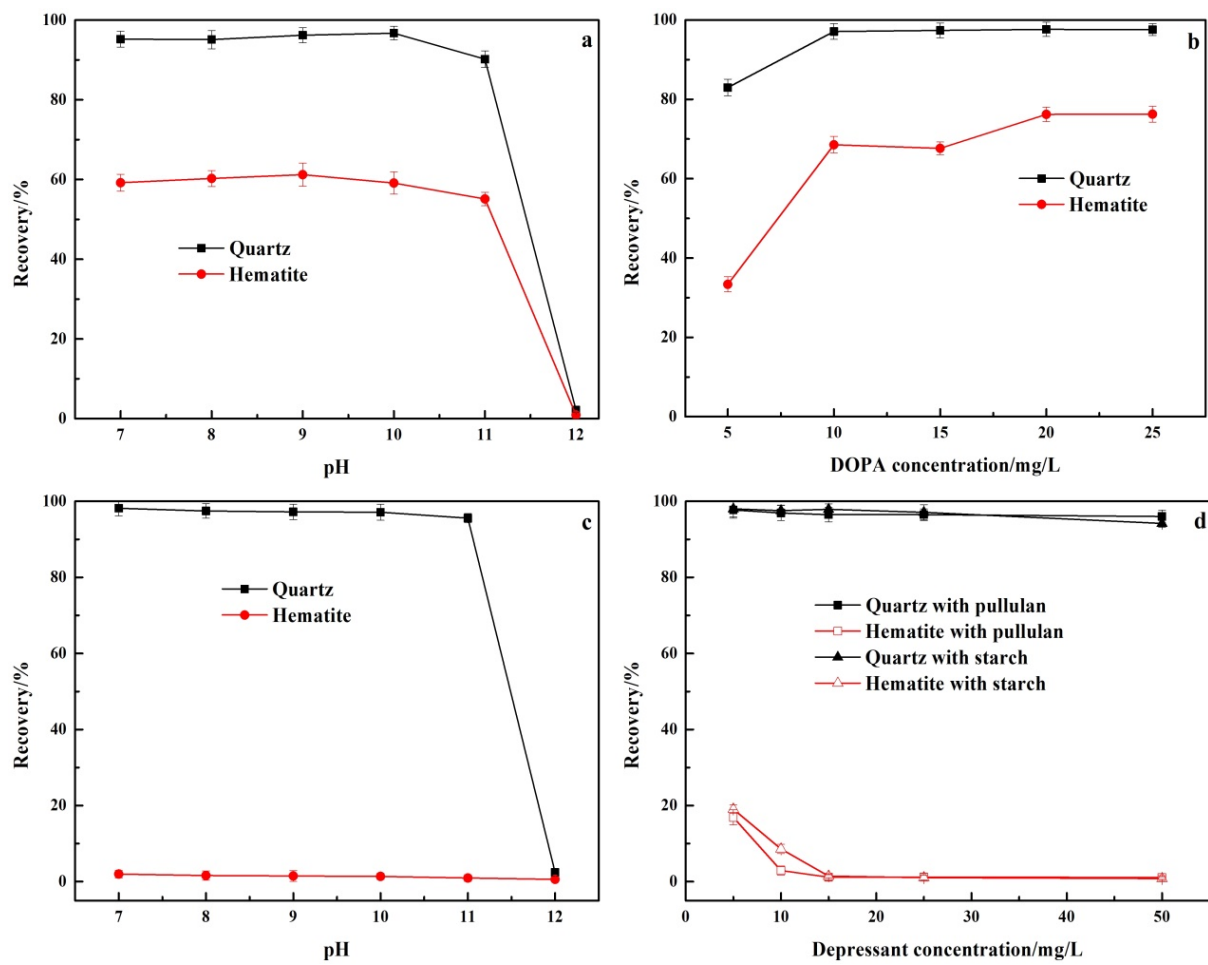


Figure 5. Effect of the addition (a,b) and absence (c,d) of pullulan and starch on the floatability of quartz and hematite. (a) DOPA concentration: 10 mg/L; pullulan: 0 mg/L; (b) pH 9, pullulan: 0 mg/L; (c) DOPA concentration: 10 mg/L; pullulan: 30 mg/L; (d) pH 9, DOPA concentration: 10 mg/L.

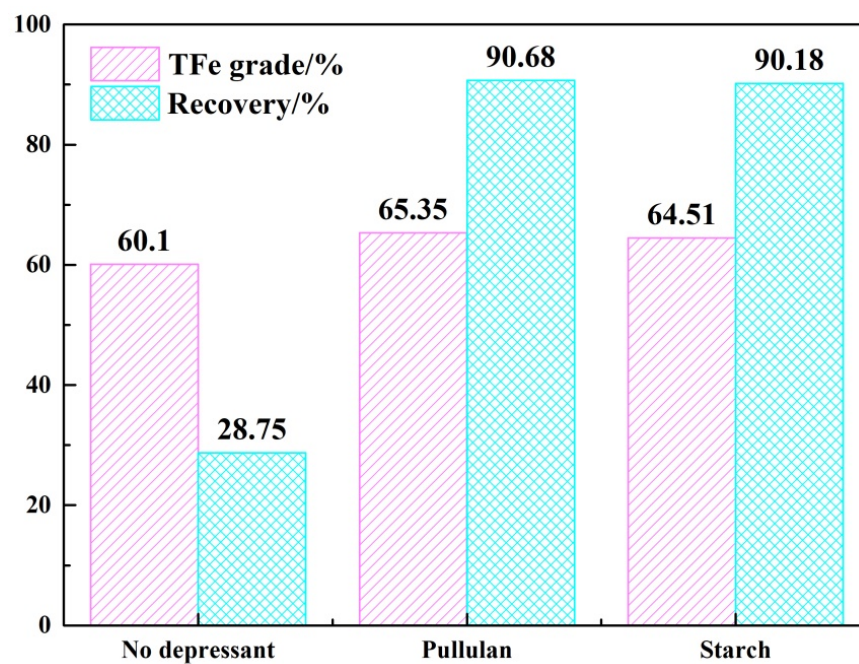


Figure 6. The results of mineral mixture tests.

3.3. Contact Angle Analyses

Flotation is to achieve the purpose of mineral separation by enlarging the hydrophobicity difference between different minerals by modifying the surface of reagents [26]. The contact angle is the most intuitive way to express the hydrophobicity of a mineral surface. The larger the contact angle, the greater the hydrophobicity [27]. As can be seen from Table 1, the contact angles of pure hematite and quartz were 29.8° and 31.2°, respectively. The contact angles of hematite and quartz increased sharply to 85.7° and 91.6° after adding collector DOPA. These results indicated that treatment with the collector DOPA increased the hydrophobicity of both minerals simultaneously. This also indicated that the addition of inhibitors was necessary. The contact angle of hematite decreased significantly after pullulan was added in advance, while the contact angle of quartz changed little, the values being 52.1° and 89.4°, respectively. After pullulan treatment, the contact angle of the hematite surface was reduced from 85.7° to 52.1°. The change in hydrophobicity of hematite and quartz after the addition of different reagents demonstrated that pullulan could be used as a selective depressant of hematite.

Table 1. Contact angle of two minerals with different reagents/°.

Test System	No Reagents	DOPA	Pullulan + DOPA
Hematite	29.8	85.7	52.1
Quartz	31.2	91.6	89.4

3.4. The Adsorption Analyses

As shown in Figure 7, with the increase of pullulan concentration, its adsorption amount on quartz and hematite surfaces increased. However, the adsorption amount of pullulan on the surface of hematite was much larger than that on the surface of quartz at the pullulan concentration of 10–50 mg/L. This showed that the adsorption capacity of pullulan to hematite was greater than that of quartz, and it is also consistent with the results of contact angle tests.

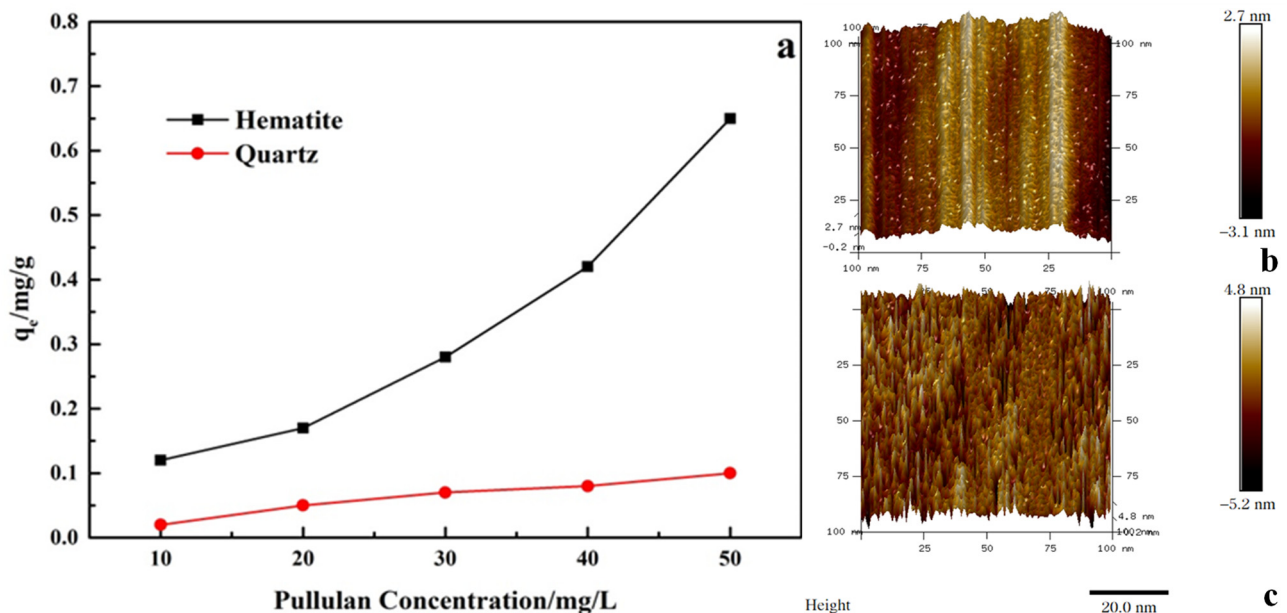


Figure 7. Adsorption capacity of pullulan on the minerals (a) and adsorption morphology of pullulan on the hematite surface (b,c).

The adsorption morphology of pullulan on hematite was further observed by atomic force microscopy. Figure 7a,b shows the AFM photographs of the hematite surface before and after the adsorption of pullulan, respectively. Figure 7b showed the natural hematite

surface with regular peaks and valleys, which were caused by the crushing process. The valleys on the surface of hematite were filled after the adsorption of pullulan, and pullulan was adsorbed on the surface of hematite in dense needle clusters. Pullulan had a large number of hydrophilic groups, and such intensive adsorption was sufficient to cause hydrophilic modification of the hematite surface.

3.5. Zeta Potential Analyses

Adsorption of reagents on the surface of minerals causes changes in the zeta potential of the mineral surface. This could help to study the adsorption mechanism of reagents with mineral surfaces [28]. The zeta potential of hematite and quartz treated with different reagents is shown in Figure 8. In Figure 8a, the isoelectric point of pure hematite was about 4.1, which had been confirmed by previous studies [11]. The zeta potential of hematite decreased significantly at pH 6–12 when pullulan was added. This indicated that pullulan could adsorb on the surface of hematite, strongly. This was due to the presence of a large number of hydroxyl groups in pullulan, which were negatively charged after dissolution, and their electronegativity increased with the increase of pH [29]. However, when DOPA was added, the zeta potential of hematite changed little. This revealed that the adsorption of pullulan on the surface of hematite prevented the adsorption of DOPA by hematite.

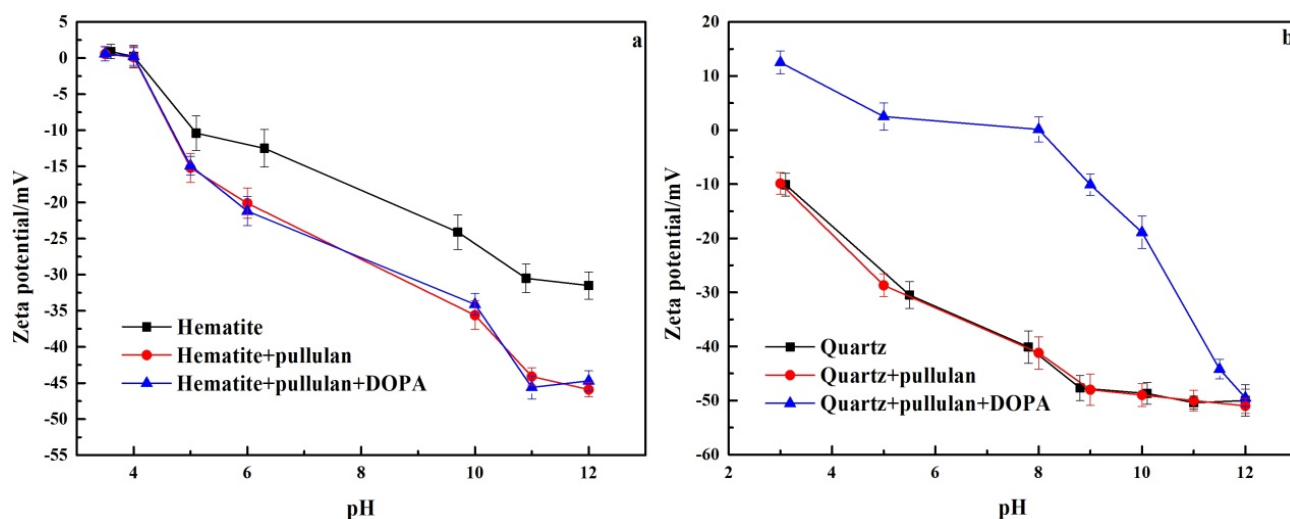


Figure 8. The zeta potential of hematite (a) and quartz (b).

As can be seen in Figure 8b, in contrast to hematite, the zeta potential of quartz had no significant change after the addition of pullulan. This demonstrated that pullulan was not adsorbed on the quartz surface. After the continued addition of DOPA, the zeta potential of quartz was significantly enhanced at pH 3–10. The increase of zeta potential on the quartz surface decreased when the pH was greater than 10, and there was almost no change at pH 12. This was because amine collectors exist in molecular form at pH 12, and are no longer adsorbed on the quartz surface by electrostatic action. This demonstrated that pullulan was not adsorbed on the quartz surface and did not affect the quartz collection by DOPA. This was the key to the separation of quartz and hematite by pullulan as a selective depressant of hematite in iron ore reverse flotation.

3.6. FT-IR Analyses

FT-IR spectroscopy is frequently used to study the characteristic adsorption of reagents on minerals. Figure 9 shows the FT-IR spectra of pure minerals and minerals treated with pullulan. The absorption spectra at 534.86 cm^{-1} and 458.69 cm^{-1} in FT-IR spectra of pure hematite were caused by the vibration of Fe–O bond of hematite [30]. The new absorption peak at 3414.56 cm^{-1} and 2922.86 cm^{-1} in the pullulan-treated hematite was attributed to the hydroxyl group (–OH) and –CH₃ of pullulan. The band of hydroxyl group

shifted from 3432.19 cm^{-1} to 3414.56 cm^{-1} , a 17.63 cm^{-1} shift. After pullulan treatment, the bands of 534.86 cm^{-1} and 458.69 cm^{-1} of pure hematite also moved to 545.16 cm^{-1} and 467.86 cm^{-1} . This indicated that chemisorption between hematite and pullulan occurred [31]. FT-IR spectra of pullulan's hematite showed an obvious pullulan absorption peak, and the hydroxyl group had a large displacement, so it was inferred that pullulan's adsorption with hematite was through hydroxyl groups.

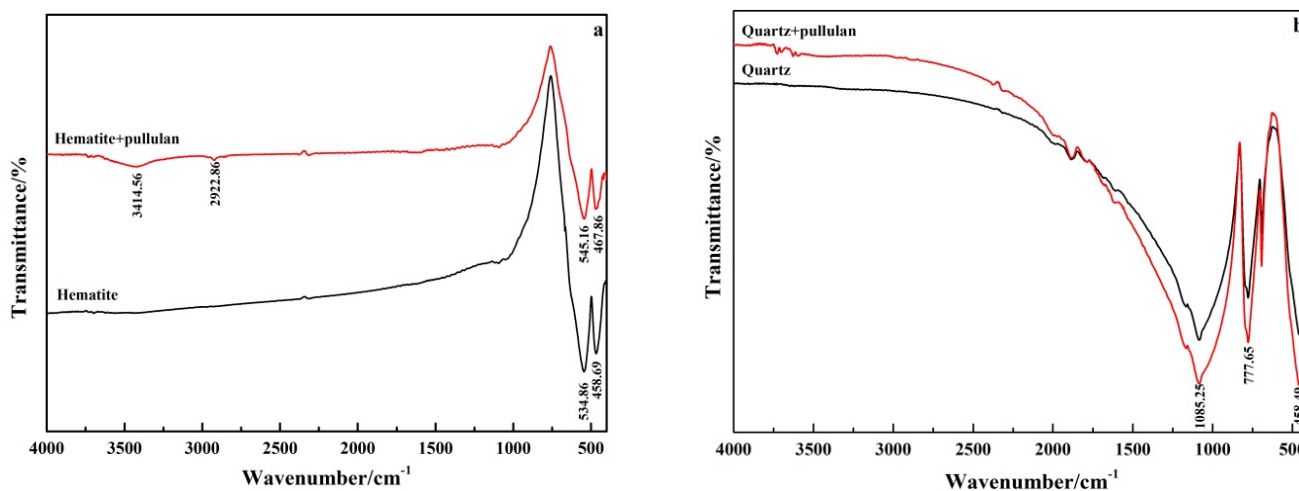


Figure 9. FT-IR spectra of hematite (a) and quartz (b) before and after pullulan treatment.

As shown in Figure 8b, the characteristic peaks of quartz were located at 458.49 cm^{-1} , 777.65 cm^{-1} and 1085.25 cm^{-1} . No new absorption peak appeared on the quartz surface treated by pullulan, and the original characteristic peak did not shift. This indicated that there was no chemisorption between quartz and pullulan. These results were consistent with zeta potential test results, which further indicated that pullulan could adsorb selectively on the surface of hematite.

3.7. XPS Analyses

In order to further reveal the adsorption mechanism between pullulan and mineral surface, XPS was used to analyze the changes of mineral surface elements before and after pullulan treatment. Table 2 shows the changes of surface elements in hematite and quartz.

Table 2. The changes of surface elements in hematite and quartz before and after pullulan treatment.

Samples	Elements/at.%				Sum/%
	C	O	Fe	Si	
Hematite	39.44	47.70	12.86	–	100
Hematite + pullulan	45.64	46.66	7.70	–	100
Shift	+6.20	−1.04	−5.16	–	
Quartz	23.55	50.56	–	25.89	100
Quartz + pullulan	24.01	50.78	–	25.21	100
Shift	+0.46	−0.22	–	−0.68	

As can be seen from Table 2, after pullulan treatment, element C on the hematite surface increased by 6.20%, while elements Fe and O decreased by 3.16% and 1.04%, respectively. Therefore, it can be inferred that there was a chemical bond between the hydroxyl group of pullulan and the iron site of hematite. The decrease of element O was caused by hydrogen bonding adsorption. The adsorption of pullulan resulted in the reduction of element Fe and element O. The elemental changes on the surface of the quartz treated with pullulan were minimal. Element C increased by 0.46%, while element O and Si decreased by 0.22% and 0.68%, respectively. This indicated that adsorption between pullulan and quartz surface

was weak. Consistent with previous work, Kumar suggested that polysaccharide inhibitors could form hydrogen bonds on quartz surfaces [32].

To further investigate the adsorption mechanism of pullulan and hematite, the C1s and O1s XPS spectra (Figure 10) of pullulan treated hematite were analyzed. Figure 10a shows the C1s spectrum of pure hematite. The carbon on the surface of pure hematite was derived from carbon contamination [33]. The peak of pullulan treated hematite was significantly enhanced at 286.33 eV (Figure 10b). The peak was due to C–OH group of pullulan and it shifted by 0.32 eV from 286.01 eV compared to pure hematite [34]. This suggested that pullulan was strongly chemically bonded by hydroxyl and hematite. Figure 10c,d show the O1s high resolution XPS spectra of pure hematite and pullulan treated hematite, respectively. In Figure 10c, the peak at 529.75 eV was oxygen in hematite Fe–O, and the peak at 531.60 eV came from oxygen in the hydroxyl group of residual water [35]. After pullulan treatment, the hydroxyl peak of hematite water weakened and a new peak appeared at 532.81 eV. The new peak was attributed to the hydroxyl group (Fe–O–C) of the pullulan bonded to the surface of the hematite [35]. XPS analyses showed that pullulan was adsorbed on hematite through a strong chemical bond between the hydroxyl group of pullulan and the Fe site of hematite.

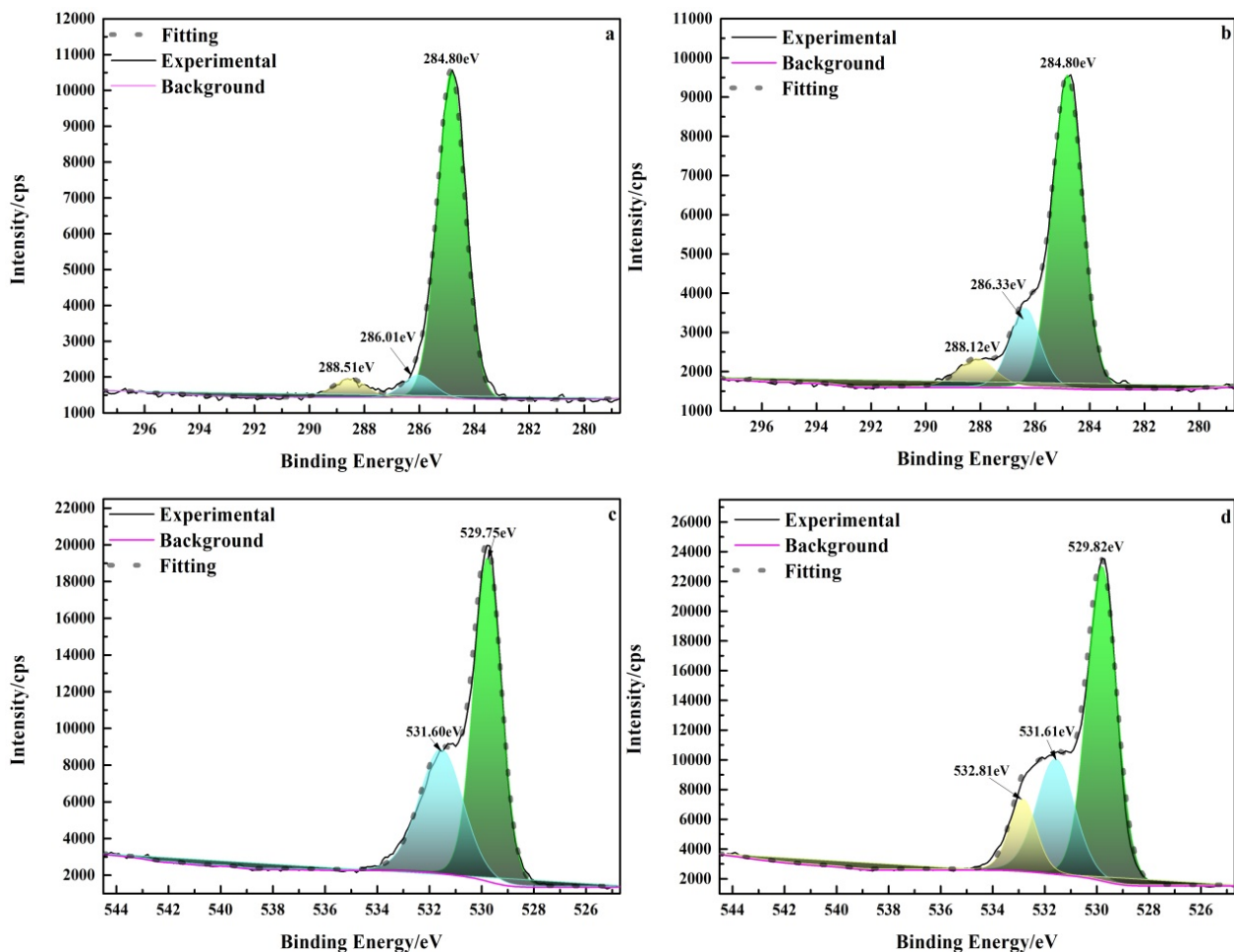


Figure 10. High-resolution XPS spectra of hematite before and after pullulan treatment. (a) C1s of hematite; (b) C1s of hematite + pullulan; (c) O1s of quartz; (d) O1s of quartz + pullulan).

Based on the analysis of the above tests, it can be inferred that pullulan chemically bonded to the Fe sites on the surface of hematite by its –OH and impeded the subsequent adsorption of DOPA. The (001) of hematite was considered to be its most easily cleaved plane [32]. The hematite fracture along the (001) plane exposed large amounts of iron

ions. Fe belongs to the d-zone elements in the periodic table of chemical elements, where coordination bonds exist. Therefore, it was possible for the iron on the surface of hematite to be chemically bonded to the hydroxyl group of pullulan. This was also consistent with the XPS analyses. Previous studies also concluded that the polysaccharide depressant starch can be chemisorbed by hematite [36]. Figure 11 shows the adsorption model of pullulan on the hematite surface.

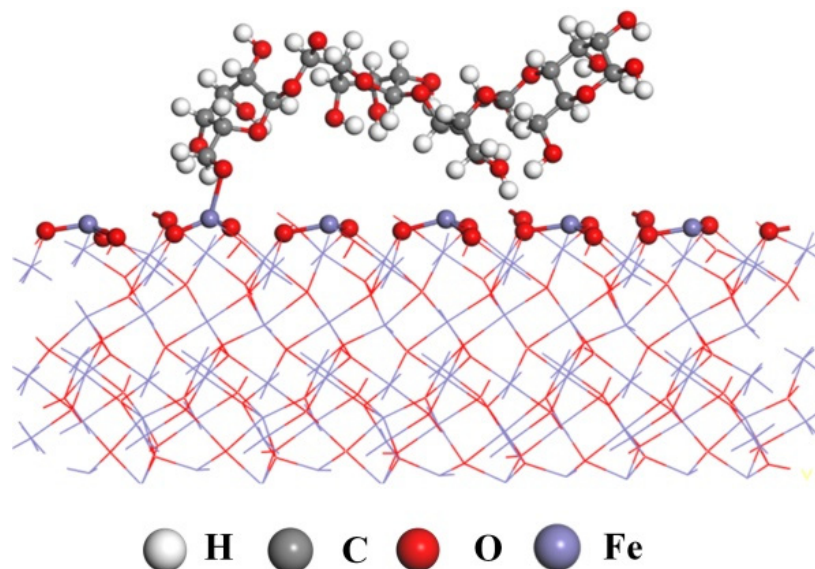


Figure 11. The pullulan adsorption model on hematite surface.

4. Conclusions

In this study, we used DOPA as collector to study the flotation behavior of pullulan, a polysaccharide depressant, on hematite and quartz and the selective depression mechanism of hematite/quartz reverse flotation. The following conclusions were reached.

1. The structure and molecular weight of pullulan were determined by the characterization of pullulan and it was found that the viscosity of pullulan was lower than that of starch, and pullulan was more suitable for flotation.
2. The single mineral flotation tests showed that pullulan had selective depression on hematite and was slightly better than starch. The iron grade of 65.35% and iron recovery of 90.68% were obtained by pullulan as depressant in mineral mixture tests, which was slightly better than starch.
3. The difference in hydrophobicity of hematite and quartz can be amplified by pre-addition of pullulan to the DOPA system to achieve their effective separation.
4. Zeta potential and FT-IR analyses showed that pullulan was selectively adsorbed on hematite and prevented the adsorption of DOPA. The weak adsorption between pullulan and quartz did not affect the hydrophobic modification of the quartz surface by DOPA.
5. XPS analyses showed that pullulan was adsorbed on the hematite surface through chemical bonding between its hydroxyl group and the Fe site on the hematite surface.

Compared with starch, pullulan was directly dissolved in cold water (no need to add high temperature or alkali to dextrinize), its viscosity was lower than that of starch, and the flotation effect was also superior to that of starch. In conclusion, pullulan was a better hematite depressant than the conventional starch depressants in terms of effectiveness and performance.

Author Contributions: Methodology, W.H., Y.Z. and Y.L.; Investigation, J.L.; Data curation, W.H. and Z.S.; Writing—original draft, W.H.; Writing—review & editing, Y.Z., Z.S., J.L. and Y.L.; Funding: Y.Z. All authors have read and agreed to the published version of the manuscript.

Funding: This study was supported by the National Natural Science Foundation of China (Grant No. 51974067 (Yimin Zhu)).

Institutional Review Board Statement: Not applicable.

Informed Consent Statement: Not applicable.

Data Availability Statement: Not applicable.

Conflicts of Interest: The authors declare no conflict of interest.

References

1. Filippov, L.; Severov, V.; Filippova, I. An overview of the beneficiation of iron ores via reverse cationic flotation. *Int. J. Miner. Process.* **2014**, *127*, 62–69. [[CrossRef](#)]
2. Li, M.; Liu, J.; Hu, Y.; Gao, X.; Yuan, Q.; Zhao, F. Investigation of the specularite/chlorite separation using chitosan as a novel depressant by direct flotation. *Carbohydr. Polym.* **2020**, *240*, 116334. [[CrossRef](#)] [[PubMed](#)]
3. Zhang, C.; Xu, Z.; Hu, Y.; He, J.; Tian, M.; Zhou, J.; Chen, S.; Sun, W. Novel Insights into the Hydroxylation Behaviors of α -Quartz (101) Surface and its Effects on the Adsorption of Sodium Oleate. *Minerals* **2019**, *9*, 450. [[CrossRef](#)]
4. Zhang, X.; Zhu, Y.; Xie, Y.; Shang, Y.; Zheng, G. A novel macromolecular depressant for reverse flotation: Synthesis and depressing mechanism in the separation of hematite and quartz. *Sep. Purif. Technol.* **2017**, *186*, 175–181. [[CrossRef](#)]
5. Wang, H.; Wang, L.; Yang, S.; Liu, C.; Xu, Y. Investigations on the reverse flotation of quartz from hematite using carboxymethyl chitosan as a depressant. *Powder Technol.* **2021**, *393*, 109–115. [[CrossRef](#)]
6. Han, W.; Zhu, Y.; Ge, W.; Liu, J.; Li, Y. Curdlan as a new depressant of hematite for quartz-hematite reverse flotation separation. *Miner. Eng.* **2022**, *185*, 107708. [[CrossRef](#)]
7. Yehia, A.; El-Halim, S.A.; Sharada, H.; Fadel, M.; Ammar, M. Application of a fungal cellulase as a green depressant of hematite in the reverse anionic flotation of a high-phosphorus iron ore. *Miner. Eng.* **2021**, *167*, 106903. [[CrossRef](#)]
8. Liu, Q.; Wannas, D.; Peng, Y. Exploiting the dual functions of polymer depressants in fine particle flotation. *Int. J. Miner. Process.* **2006**, *80*, 244–254. [[CrossRef](#)]
9. Turrer, H.; Peres, A. Investigation on alternative depressants for iron ore flotation. *Miner. Eng.* **2010**, *23*, 1066–1069. [[CrossRef](#)]
10. Tohry, A.; Dehghan, R.; Zarei, M.; Chelgani, S.C. Mechanism of humic acid adsorption as a flotation separation depressant on the complex silicates and hematite. *Miner. Eng.* **2020**, *162*, 106736. [[CrossRef](#)]
11. Han, W.; Zhu, Y.; Liu, J.; Li, Y. A novel depressant HPAM of the hematite in reverse cationic flotation of iron ore. *Colloids Surf. A Physicochem. Eng. Asp.* **2022**, *641*, 128547. [[CrossRef](#)]
12. Krawczyk, H.; Arkell, A.; Jönsson, A.-S. Membrane performance during ultrafiltration of a high-viscosity solution containing hemicelluloses from wheat bran. *Sep. Purif. Technol.* **2011**, *83*, 144–150. [[CrossRef](#)]
13. Alhomodi, A.F.; Gibbons, W.R.; Karki, B. Estimation of cellulase production by *Aureobasidium pullulans*, *Neurospora crassa*, and *Trichoderma reesei* during solid and submerged state fermentation of raw and processed canola meal. *Bioresour. Technol. Rep.* **2022**, *18*, 101063. [[CrossRef](#)]
14. Haghighatpanah, N.; Khodaiyan, F.; Kennedy, J.F.; Hosseini, S.S. Optimization and characterization of pullulan obtained from corn bran hydrolysates by *Aerobasidium pullulans* KY767024. *Biocatal. Agric. Biotechnol.* **2021**, *33*, 101959. [[CrossRef](#)]
15. Cui, Y.; Jiao, F.; Qin, W.; Wang, C.; Li, X. Flotation separation of sphalerite from galena using eco-friendly and efficient depressant pullulan. *Sep. Purif. Technol.* **2022**, *295*, 121013. [[CrossRef](#)]
16. Ning, S.; Li, G.; Shen, P.; Zhang, X.; Li, J.; Liu, R.; Liu, D. Selective separation of chalcopyrite and talc using pullulan as a new depressant. *Colloids Surf. A Physicochem. Eng. Asp.* **2021**, *623*, 126764. [[CrossRef](#)]
17. Singh, R.S.; Saini, G.K.; Kennedy, J.F. Downstream processing and characterization of pullulan from a novel colour variant strain of *Aureobasidium pullulans* FB-1. *Carbohydr. Polym.* **2009**, *78*, 89–94. [[CrossRef](#)]
18. Pieleś, A.; Biniś, W.; Paluch, J. Mild acid hydrolysis of fucoidan: Characterization by electrophoresis and FT-Raman spectroscopy. *Carbohydr. Res.* **2011**, *346*, 1937–1944. [[CrossRef](#)]
19. Wiercigroch, E.; Szafraniec, E.; Czamara, K.; Pacia, M.Z.; Majzner, K.; Kochan, K.; Kaczor, A.; Baranska, M.; Malek, K. Raman and infrared spectroscopy of carbohydrates: A review. *Spectrochim. Acta Part A Mol. Biomol. Spectrosc.* **2017**, *185*, 317–335. [[CrossRef](#)]
20. Kacuráková, M.; Capek, P.; Sasinková, V.; Wellner, N.; Ebringerová, A. FT-IR study of plant cell wall model compounds: Pectic polysaccharides and hemicelluloses. *Carbohydr. Polym.* **2000**, *43*, 195–203. [[CrossRef](#)]
21. Bai, W.; Shah, F.; Wang, Q.; Liu, H. Dissolution, regeneration and characterization of curdlan in the ionic liquid 1-ethyl-3-methylimidazolium acetate. *Int. J. Biol. Macromol.* **2019**, *130*, 922–927. [[CrossRef](#)] [[PubMed](#)]
22. McFadzean, B.; Groenmeyer, G. Selective molecular weight adsorption from polydisperse polysaccharide depressants. *Miner. Eng.* **2015**, *77*, 172–178. [[CrossRef](#)]
23. McFadzean, B.; Dicks, P.; Groenmeyer, G.; Harris, P.; O'Connor, C. The effect of molecular weight on the adsorption and efficacy of polysaccharide depressants. *Miner. Eng.* **2011**, *24*, 463–469. [[CrossRef](#)]
24. Iwasaki, I.; Cooke, S.; Colombo, A.F. Flotation characteristics of goethite. In *Flotation Characteristics of Goethite*; U.S. Department of the Interior, Bureau of Mines: Washington, DC, USA, 1960.
25. Smith, R.W.; Scott, J.L. Mechanisms of Dodecylamine Flotation of Quartz. *Miner. Process. Extr. Met. Rev.* **1990**, *7*, 81–94. [[CrossRef](#)]

26. Hao, H.; Li, L.; Yuan, Z.; Patra, P.; Somasundaran, P. Adsorption differences of sodium oleate on siderite and hematite. *Miner. Eng.* **2019**, *137*, 10–18. [[CrossRef](#)]
27. Wang, C.; Liu, R.; Wu, M.; Zhai, Q.; Luo, Y.; Jing, N.; Xie, F.; Sun, W. Selective separation of chalcopyrite from sphalerite with a novel depressant fenugreek gum: Flotation and adsorption mechanism. *Miner. Eng.* **2022**, *184*, 107653. [[CrossRef](#)]
28. Zhou, H.; Yang, Z.; Zhang, Y.; Sun, W.; Gao, Z.; Lei, M. Effect of *Artemisia sphaerocephala* Krasch. Gum on the flotation separation of fluorite from calcite. *Miner. Eng.* **2021**, *174*, 107249. [[CrossRef](#)]
29. Zhou, H.; Yang, Z.; Tang, X.; Sun, W.; Gao, Z.; Luo, X. Enhancing flotation separation effect of fluorite and calcite with polysaccharide depressant tamarind seed gum. *Colloids Surf. A Physicochem. Eng. Asp.* **2021**, *624*, 126784. [[CrossRef](#)]
30. Tohry, A.; Dehghan, R.; Filho, L.D.S.L.; Chelgani, S.C. Tannin: An eco-friendly depressant for the green flotation separation of hematite from quartz. *Miner. Eng.* **2021**, *168*, 106917. [[CrossRef](#)]
31. Espiritu, E.R.L.; Naseri, S.; Waters, K.E. Surface chemistry and flotation behavior of dolomite, monazite and bastnäsite in the presence of benzohydroxamate, sodium oleate and phosphoric acid ester collectors. *Colloids Surf. A Physicochem. Eng. Asp.* **2018**, *546*, 254–265. [[CrossRef](#)]
32. Kumar, D.; Jain, V.; Rai, B. Can carboxymethyl cellulose be used as a selective flocculant for beneficiating alumina-rich iron ore slimes? A density functional theory and experimental study. *Miner. Eng.* **2018**, *121*, 47–54. [[CrossRef](#)]
33. Cheng, K.; Wu, X.; Tang, H.; Zeng, Y. The flotation of fine hematite by selective flocculation using sodium polyacrylate. *Miner. Eng.* **2021**, *176*, 107273. [[CrossRef](#)]
34. Moreira, G.F.; Peçanha, E.R.; Monte, M.B.; Filho, L.S.L.; Stavale, F. XPS study on the mechanism of starch-hematite surface chemical complexation. *Miner. Eng.* **2017**, *110*, 96–103. [[CrossRef](#)]
35. Hacha, R.R.; LeonardoTorem, M.; Merma, A.G.; Coelho, V.F.D.S. Electroflotation of fine hematite particles with *Rhodococcus opacus* as a biocollector in a modified Partridge–Smith cell. *Miner. Eng.* **2018**, *126*, 105–115. [[CrossRef](#)]
36. Li, L.; Zhang, C.; Yuan, Z.; Xu, X.; Song, Z. AFM and DFT study of depression of hematite in oleate-starch-hematite flotation system. *Appl. Surf. Sci.* **2019**, *480*, 749–758. [[CrossRef](#)]

Disclaimer/Publisher’s Note: The statements, opinions and data contained in all publications are solely those of the individual author(s) and contributor(s) and not of MDPI and/or the editor(s). MDPI and/or the editor(s) disclaim responsibility for any injury to people or property resulting from any ideas, methods, instructions or products referred to in the content.